Ephemeris Generation for ETS-VI and Its Effects on Pointing Strategies Adopted for Daytime Acquisition and Tracking

W. M. Owen, Jr.
Navigation and Flight Mechanics Section

S. D. Gillam, J. W. Young, and D. L. Mayes
Earth and Space Sciences Division

Critical to the success of the Ground/Orbiter Lasercomm Demonstration (GOLD) was the ability of the two telescopes at the Table Mountain Facility (TMF) to track the Japanese Engineering Test Satellite (ETS-VI). This article describes the process of generating pointing predictions from the satellite's orbital elements, experiments to determine the inherent pointing accuracy of the TMF telescopes, and the strategies developed for overcoming errors in the satellite's ephemeris. The combination of ephemeris precision, telescope-pointing precision, and low satellite contrast against the bright sky made daytime satellite acquisition a serious challenge. Inherent telescope-pointing error in right ascension, end play in the declination axis worm gear, and pointing error induced by the statistical errors in the ephemeris were thought to be the main sources of error in the telescope pointing.

I. Introduction

The ability of the two telescopes at JPL's Table Mountain Facility (TMF) to point accurately at the Japanese Engineering Test Satellite (ETS-VI) was necessary for the Ground/Orbiter Lasercomm Demonstration (GOLD) [1] to be a success. The 0.6-m telescope, used for transmitting the uplink laser beacon, had to be pointed to an accuracy smaller than the 30-μrad (6-arcsec) beamwidth of the laser; otherwise the light from the laser would not intercept the satellite. Similarly, the 1.2-m telescope, used for detecting the return signal from the ETS-VI, had to track well enough to ensure that the satellite always appeared in the receiver's 80-μrad field of view.

There are two parts to the problem. The first part is the production of two "tracking files," one for each telescope, that contain tables giving the apparent topocentric pointing direction at regular time intervals. These files, based on orbital elements determined by the Japanese National Aeronautics and Space Development Agency (NASDA), were produced a day or two before each experiment and transferred to the computers that control the telescopes. The second part is the real-time control of each telescope. Because the orbital elements carried a statistical uncertainty, the predicted pointing directions rarely were accurate enough to be used unchanged. Strategies had to be developed to find the ETS-VI and to cope with any drifts in the tracking over the hours of each experiment.

II. Production of Tracking Files

The process of generating tracking files for the two telescopes at TMF began with the receipt of an orbit solution from NASDA. These solutions were generated roughly twice each week during the lifetime of the ETS-VI. They were transmitted by fax during Phase I of GOLD and by e-mail during Phase II. Each transmission contained a set of osculating orbital elements (semimajor axis, eccentricity, inclination, right ascension of the ascending node, argument of perigee, and both mean and true anomaly) as well as the corresponding components of the position and velocity vectors at the UTC epoch of the solution. The elements and the state vector were given twice: once referred to the Earth mean equator and equinox of 2000.0 (J2000 coordinates) and once referred to the Earth true equator and equinox of date (true-of-date coordinates). These two representations of the same solution differ only in their coordinate system, and one can move from one to the other by applying the standard International Astronomical Union (IAU) precession and nutation rotation matrices. The J2000 version, being inertial, was adopted for subsequent processing.

NASDA supplied an estimate of the position and velocity of the ETS-VI at a specified time. The Navigation and Flight Mechanics Section's DPTRAJ program[1] was then used to integrate the spacecraft's trajectory. Since the velocity components were given only to six or seven significant digits, it was better to convert the orbital elements (which carried greater precision) into position and velocity. This conversion process also provided a way of ensuring that the elements and vectors from NASDA were in agreement. The integration itself used the default force model for Earth orbiters: perturbations from the Sun and Moon, a 12-by-12 gravity field for the Earth, solar radiation pressure, and relativity effects. Atmospheric drag was not a concern because the satellite never entered within the 2000-km height of the model atmosphere.

The result of the integration was a trajectory file, spanning several weeks, that could be interpolated to find the J2000 geocentric position and velocity of the ETS-VI at any desired time. The tracking files used at the telescopes, however, had to contain tables of apparent topocentric right ascension and declination. There had to be different files for the two telescopes, partly because of the distance between them, but mostly because the uplink and downlink directions differ due to light-time and stellar aberration effects.

The tracking files were created by TCPEPH, a program written specifically for the GOLD demonstration. TCPEPH is based in part on an earlier program written for the Galileo Optical Experiment (GOPEX) [2] and in part on the prediction capabilities of the Optical Navigation Program [3].

For downlink files, TCPEPH performs the same set of calculations that is used for any solar system object. First, the position and velocity of the telescope are found relative to the solar system barycenter: the geocentric body-fixed coordinates are rotated into J2000 by accounting for precession, nutation, Greenwich sidereal time, and polar motion, and the resulting vectors are added to the position and velocity of the Earth as interpolated from planetary ephemeris DE403.[2] Second, the position of the ETS-VI is found from the spacecraft trajectory file and likewise referred to the solar system barycenter. The difference between these two position vectors is the geometric position of the ETS-VI relative to the telescope. The light time from the ETS-VI to the telescope is found, and the barycentric position of the ETS-VI is interpolated at the retarded time when the light left it. This step is iterated until convergence. The true position thus found is corrected for stellar aberration, yielding the apparent position, and then rotated from J2000 into true-of-date coordinates.

The calculations for uplink files [2] are subtly different. One begins again with the state of both the telescope and the ETS-VI at the desired time, but this time one must find the barycentric position of the

---

[1] J. E. Ekelund, V. N. Legerton, L. R. Stavert, R. F. Sunseri, and T.-C. Wang, *DPTRAJ-ODP User's Reference Manual*, Mars Global Surveyor Project 642-3405-DPTRAJ-ODP (internal document), Jet Propulsion Laboratory, Pasadena, California, March 22, 1996.

[2] E. M. Standish, "DE403/LE403: Announcement," JPL Interoffice Memorandum 314.10-124 (internal document), Jet Propulsion Laboratory, Pasadena, California, May 8, 1995.

ETS-VI after the desired time, i.e., when light emitted at the telescope would intercept the satellite. The correction for stellar aberration likewise is applied in the opposite sense.

Consequently, the uplink and downlink directions are different, even for the same telescope; the difference for the ETS-VI could amount to 100 μrad near perigee, which is greater than the beamwidth of the laser. Pointing the telescope at the apparent position of the satellite (as seen by reflected sunlight) would cause the uplink laser to miss the satellite altogether. Yet it was necessary to use reflected sunlight to find the satellite initially and to monitor the pointing of the telescope during the experiment. Consequently, an auxiliary file was generated that gave the difference between the uplink and downlink directions.

The tracking files were limited to 2000 entries. Precursor experiments in which the telescope tracked the ETS-VI without transmitting verified that the tracking was adequate with 1-min intervals between entries. An entire 14-hour pass could then fit in one tracking file. The tracking files and the auxiliary offset file were generated at the Oak Grove site and transferred by the Internet to one of the computers resident at the TMF, where the files were written to diskette and copied onto the computers that actually control the two telescopes. Whenever a solution was received, files would be created for the next two passes. This policy provided a backup in case a solution was bad or the Internet connection went down.

III. Pointing Strategies for the Transmitter Telescope

A PulNix DN-007F3 intensified charge-coupled device (CCD) video camera was used at the coudé focus for nighttime satellite acquisition in the Phase-1 demonstration [4]. We used the same camera for pointing-calibration tests. The pointing of the 0.6-m telescope was found to suffer from accumulated errors on the order of 0.5 to 1.0 arcsec/deg of slew. Initially, this resulted in the need to search a box on the sky of from 0.25 to 1.0 deg^2 in order to acquire the satellite. These errors were very evident on May 5, 1996. Calibration was performed on a star 30 deg from the satellite position. The satellite was acquired 3 arcsec in right ascension and 34 arcsec in declination from the center of the field of view of the acquisition camera. Experiments were performed later that night using the same ephemeris and another star approximately 30 deg from the satellite. The declination pointing error was 34 arcsec, and the right ascension error was 21 arcsec. Another positional calibration using a star 5 deg from the satellite reduced the pointing error to 5 arcsec. Subsequently, pointing calibration was performed using stars located along the satellite track in order to minimize the distance moved to the ETS-VI and to minimize the size of the search box. In daylight, only red stars brighter than $m_V = 6.0$ were detectable at the transmitter. This limited stars suitable for daytime positional calibration to the list given in Table 1. In Table 1, the "$\alpha(2000.0)$" and "$\delta(2000.0)$" columns give the right ascension and declination coordinates, respectively, of the star referred to the Earth mean equator and equinox of 2000.0. The "Class" column gives the spectral class of the star; B and G stars are bluer in color than K and M stars. The "m_v" column indicates the relative brightness of each star on a logarithmic scale; the more positive the number, the fainter the star. The brightest in this table is α Leo, and the faintest is 56 Leonis. Once the satellite was acquired, continuous tracking was performed in the same way as for nighttime satellite tracking [4].

Because the transmitter occasionally was shared with other users throughout the GOLD experiment [4], the start of every tracking run began with positional calibration with α Leonis (α Leo) as the reference. It can be seen from Table 1 that α Leo is a very bright and unmistakable star. This made it ideal as a primary positional standard, even during the day. This star was close to the beginning of the satellite track in the middle of March (the beginning of the daytime GOLD experiment) and, subsequently, became the prime calibration star used throughout the remainder of the GOLD demonstration. The receiver and transmitter were calibrated to this star at the same time. By mid-April, the satellite rose before sunset, because of the motion of the Earth around the Sun. It also moved further away from the position of α Leo in the sky on each successive pass. By mid-April, the red stars in Table 1 were needed for positional calibration.

The PulNix camera had an extended red sensitivity that aided the detection of redder stars. An RG-7 3-mm-thick Schott glass filter was placed in front of the camera to attenuate the light from the blue sky.

Table 1. Stars used for daytime positional calibration of the telescopes [5].

No.	Name	α (2000.0)	δ (2000.0)	Class	m_v
		hh mm ss	d mm ss		
1	α Leo	10 08 22	11 58 02	B7	1.35
2	44 Leo	10 25 15	8 47 06	Ma	5.61
3	48 Leo	10 34 48	6 57 14	G8	5.08
4	56 Leo	10 56 01	6 11 07	M5	5.81
5	d Leo	11 00 34	3 37 03	K1	4.84
6	p^4 Leo	11 06 54	1 57 20	G7	5.52
7	75 Leo	11 17 17	2 00 37	M0	5.18
8	τ Leo	11 27 56	2 51 22	G8	4.95
9	ω Vir	11 38 28	8 08 03	M6	5.36
10	ν Vir	11 45 41	6 32 56	M1	4.03
11	o Vir	12 05 13	8 43 59	G8	4.12
12	c Vir	12 20 21	3 18 45	K0	4.96
13	δ Vir	12 55 36	3 23 51	M3	3.38
14	σ Vir	13 17 26	5 29 18	M1	4.80

This also aided the detection of faint red stars. A remotely controlled shutter was placed between the uplink laser beam and the 0.6-m telescope. When closed, this shutter prevented scattered green light (514 nm) from the laser from entering the PulNix camera. When the satellite was visible, this allowed the telescope operator to switch rapidly between the uplink transmission and visual verification of the position of the ETS-VI in the field of view.

There were times when the satellite was not immediately detected in the field of view of the PulNiX camera. On these occasions, an expanding spiral search pattern was used to locate it. This pattern consisted of 3-arcsec steps and dwelling at each position for 4 seconds. This process usually took 20 min. The ETS-VI occasionally was found up to an arcminute from the predicted position.

IV. Pointing Strategies at the Receiver Telescope

Two cameras were available at the 1.2-m telescope for visual acquisition of calibration stars and the ETS-VI. A Cohu video camera was mounted at the focus of a 0.4-m finder telescope attached to the body of the main telescope. This camera had a field of view of 6 arcmin by 6 arcmin. An intensified SpectraSource Lynxx slow-scan CCD camera was included as part of the GOLD receiver assembly [4], which was mounted at the Cassegrain focus of the 1.2-m telescope. The Lynxx had a field of view of 17 arcsec by 15 arcsec. The field of view of the Cohu camera allowed rapid but less precise acquisition of the calibration stars. It was limited to very bright stars and could not detect the ETS-VI when the satellite was not illuminated by the downlink laser. A red 6-mm RG-7 glass filter was placed in front of the Cohu camera to increase the contrast between stars and the blue sky. As at the transmitter, this made necessary the choice of red stars for positional calibration standards.

The 1.2-m telescope lacked the tube and optical baffling of the 0.6-m telescope, which allowed light scattered from the surroundings to reach the Lynxx camera. The Lynxx also lacked the extended red sensitivity of the PulNiX camera at the transmitter, and a red filter was not placed in front of it. The lack of red sensitivity, the absence of a red filter, and the presence of light scattered into the line of sight limited the list of calibrators visible to this system to red stars no fainter than $m_v = 2.6$.

Many attempts were made to acquire the satellite at the receiver using reflected sunlight only. Most of them were not successful until the sun had set, because the daytime sky brightness made the satellite virtually invisible. However, daytime acquisition of the ETS-VI at the receiver was almost trivial if the downlink laser was turned on, because it was bright enough to be seen in the daytime sky. This required that the uplink be established first. Fine adjustments to the receiver pointing were then made by peaking up the downlink signal on the avalanche photodiode that detected the downlink telemetry.

V. Experiments to Determine Ephemeris Precision

On the night of May 15, 1996 UT, a scheduling conflict precluded DSN support of GOLD. Two series of experiments were performed at both the 0.6-m and the 1.2-m telescopes in an attempt to determine two things at each site. These were the degree to which the inherent pointing accuracy of the telescope and errors in the ephemeris affected pointing to the satellite. It should be noted here that there is no practical difference between tracking and pointing at the 0.6-m or the 1.2-m telescope. This is because tracking an object with the telescope control program is just a matter of continually repointing the telescopes in real time. The instantaneous tracking rate is dependent on an estimate of the first derivative of the instantaneous change in position.[3]

The inherent pointing accuracy of the 0.6-meter telescope's overslews that would be typical of daytime satellite acquisition were measured in the following way: The 0.6-m telescope was positionally calibrated [4] on star 1 in Table 2. It was then slewed to star 2. The offsets, in right ascension and declination, required to center star 2 in the field of view of the telescope were recorded. The offsets were then removed, the telescope recalibrated on star 1, and moved to star 3. Centering offsets again were recorded. This procedure was repeated for stars 4 and 5 in Table 2. The star-to-star slews varied between 0 and 29 deg in right ascension and between 0 and 5 deg in declination. In Table 2, the first column contains the star number, the second column the name, and the third and fourth columns the right ascension and declination coordinates, respectively, of the position on July 2, 1996 UT (1996.5). These positions differ by approximately 2.5 arcsec in declination from their positions on May 15, 1996.

Table 2. Stars used for the pointing tests.

No.	Name	α (1996.5)	δ (1996.5)	Class	m_v
		hh mm ss	d mm ss		
1	o Vir	12 05 02	8 45 09	G8	4.12
2	ρ Vir	12 41 42	10 15 17	A0	4.88
3	ε Vir	13 02 00	10 58 40	G8	2.83
4	78 Vir	13 33 57	3 40 37	A1	4.94
5	HR 5270	14 02 22	9 42 11	G8	6.20

The accuracy with which the 0.6-m telescope could be pointed at the satellite was determined in the following way: The telescope was calibrated on star 1 and then slewed to the satellite. The offsets required to center it in the field of view of the camera were estimated as before. These offsets were then removed and the telescope moved to star 2. Positional calibration was performed on this star and the telescope slewed to the satellite. Centering offsets again were estimated and recorded. This procedure was repeated for stars 3, 4, and 5. The star-to-satellite slews varied between 0.7 and 25 deg in right ascension and between 3 and 10 deg in declination. Each of the above slews was repeated three times. The results appear in Tables 3 and 4, where the first column contains the number of the star slewed to or from, respectively, and the second and third contain the distances slewed in right ascension and

[3] G. L. Grasdalen, personal communication, G-Star Enterprises, Denver, Colorado, 1996.

Table 3. Results of the star-to-star experiments at the 0.6-m telescope.

No.	$\Delta\alpha$, deg	$\Delta\delta$, deg	$\varepsilon(\alpha)$, arcsec	$\varepsilon(\delta)$, arcsec	Total, arcsec
1	0.000	0.000	0.0	0.0	0.0
2	8.238	1.502	23.6	7.6	24.8
3	12.777	2.225	29.6	8.8	30.9
4	23.923	−5.076	46.8	4.8	47.0
5	28.430	−0.951	55.6	11.6	57.0
1	0.000	0.000	0.0	0.0	0.0
2	8.238	1.502	22.4	6.8	23.4
3	12.777	2.225	31.6	3.2	31.8
4	23.923	5.076	49.2	4.8	49.4
5	28.430	0.951	52.4	12.0	53.8
1	0.000	0.000	0.0	0.0	0.0
2	8.238	1.502	15.6	5.6	16.6
3	12.777	2.225	32.8	3.6	33.0
4	23.923	−5.076	46.4	2.8	46.5
5	28.430	0.951	58.4	9.2	59.1

Table 4. Results of the star-to-satellite experiments at the 0.6-m telescope.

No.	$\Delta\alpha$, deg	$\Delta\delta$, deg	$\varepsilon(\alpha)$, arcsec	$\varepsilon(\delta)$, arcsec	Total, arcsec
1	25.053	−7.852	23.6	3.6	23.9
2	18.077	−9.721	15.6	−4.0	16.1
3	13.789	−10.611	9.6	−3.6	10.3
4	3.328	−3.444	−29.6	2.4	29.7
5	−0.681	−9.620	−31.6	−5.2	32.0
1	32.715	−10.202	27.2	10.4	29.1
2	25.056	−11.905	20.0	−0.8	20.0
3	21.086	−12.828	14.8	1.2	14.8
4	10.429	−5.677	1.2	6.0	6.1
5	6.382	−11.870	−17.2	−6.0	18.2
1	35.703	−11.202	30.0	10.4	31.8
2	28.104	−12.938	22.4	1.6	22.5
3	24.285	−13.911	20.8	4.0	21.1
4	13.710	−6.810	3.2	2.4	4.0
5	9.738	−13.020	−3.2	−3.2	4.5

declination, respectively. These are in the sense of $\Delta\alpha_i = \alpha_i - \alpha_1$ and $\Delta\delta_i = \delta_i - \delta_1$ for Table 3 and $\Delta\alpha_i = \alpha_{\rm satellite} - \alpha_i$ and $\Delta\delta_i = \delta_{\rm satellite} - \delta_i$ for Table 4. They are calculated from the coordinates given in Table 2, and the satellite positions for Table 4 were taken from the Telescope Control Program (TCP) screen at the time of the slew. The fourth and fifth columns contain the pointing corrections made to center the star in the field of view of the PulNiX camera. The sixth column is the total correction to center the star, calculated from the fourth and fifth columns.

The same experiments were performed at the 1.2-m telescope at the same time. In this case, offsets were recorded in terms of track and cross-track angles. In both cases, offsets were recorded in terms of the coordinate system defined by the telescope mount. These are described in [4]. The results are summarized in Tables 5 and 6, where columns one through three are as in Tables 3 and 4 and the fourth and fifth columns contain the pointing corrections made to center the star in the field of view of the Lynxx camera. These were recorded in track (tr) and cross-track (xtr) coordinates. This coordinate system was defined by the 1.2-m telescope mount, whose pole points at the zenith and not at the pole of the celestial coordinate system. This means that all corrective motions were applied in track and cross-track. The sixth column is the total correction to center the star, calculated from the fourth and fifth columns.

Table 5. Results of the star-to-star experiments at the 1.2-m telescope.

No.	$\Delta\alpha$, deg	$\Delta\delta$, deg	$\varepsilon(tr)$, arcsec	$\varepsilon(xtr)$, arcsec	Total, arcsec
1	0.000	0.000	0.0	0.0	0.0
2	8.238	1.502	−8.0	0.0	8.0
3	12.777	2.225	−7.0	0.0	7.0
4	23.923	−5.076	−1.0	7.0	7.0
5	28.430	0.951	−6.0	3.0	7.0
1	0.000	0.000	0.0	0.0	0.0
2	8.238	1.502	6.0	0.0	6.0
3	12.777	2.225	−6.0	−3.0	7.0
4	23.923	−5.076	0.0	4.0	4.0
5	28.430	0.951	−2.0	0.0	2.0
1	0.000	0.000	0.0	0.0	0.0
2	8.238	1.502	0.0	−2.0	2.0
3	12.777	2.225	−4.0	−2.0	5.0
4	23.923	−5.076	0.0	4.0	4.0
5	28.430	0.951	−3.0	0.0	3.0

The pointing accuracy of the 0.6-m telescope in the right ascension direction was examined by plotting $\varepsilon(\alpha)$ against $\Delta\alpha$ from Table 3. A plot of $\varepsilon(\delta)$ against $\Delta\delta$ gave an indication of the pointing accuracy of the 0.6-m telescope in the declination direction. Similar plots from Table 4 indicate how well the telescope was able to point at the satellite. These are shown in Figs. 1(a) through 1(d). Plots of $\varepsilon(tr)$ against $\Delta\alpha$ and of $\varepsilon(xtr)$ against $\Delta\delta$ from Tables 5 and 6 indicate the pointing accuracy of the 1.2-m telescope when tracking sidereally and when following its ETS-VI ephemeris for that night. These are shown in Figs 2(a) through 2(d).

Figure 1(a) shows clearly that the pointing errors in right ascension (RA) increased monotonically with the slew distance. The cause of these errors is still under investigation. Figure 1(b) shows a similar trend in right ascension pointing errors when slewing to the satellite. Subtracting the curve in Fig. 1(a) from that in Fig. 1(b) leaves a nearly constant residual of approximately −30 arcsec. Thus, an error not related to the inherent 0.6-m telescope pointing caused the telescope to overshoot the satellite position by about 30 arcsec. This overshoot was independent of slew distance in right ascension. Figure 1(c) does not show a clear relationship between pointing offsets and slew distance in declination (DEC). The telescope consistently undershot the desired position. This is indicated by the consistently positive declination corrections shown in Fig. 1(c).

Table 6. Results of the star-to-satellite experiments at the 1.2-m telescope.

No.	$\Delta\alpha$, deg	$\Delta\delta$, deg	$\varepsilon(tr)$, arcsec	$\varepsilon(xtr)$, arcsec	Total, arcsec
1	24.927	−6.581	−39.0	3.0	39.0
2	19.071	−9.629	−41.0	9.0	42.0
3	15.164	−9.372	−46.0	6.0	46.0
4	5.921	−2.823	−43.0	2.0	43.0
5	2.567	−9.514	−42.0	8.0	43.0
1	32.841	−8.997	−50.0	0.0	50.0
2	26.646	−12.062	−46.0	8.0	47.0
3	22.891	−11.922	−55.0	1.0	56.0
4	15.205	−6.090	−54.0	4.0	54.0
5	13.268	−13.297	−49.0	6.0	49.0
1	44.476	−13.198	−60.0	−4.0	60.0
2	39.540	−16.895	−57.0	2.0	57.0
3	36.774	−17.256	−53.0	2.0	53.0
4	30.220	−12.123	−51.0	0.0	51.0

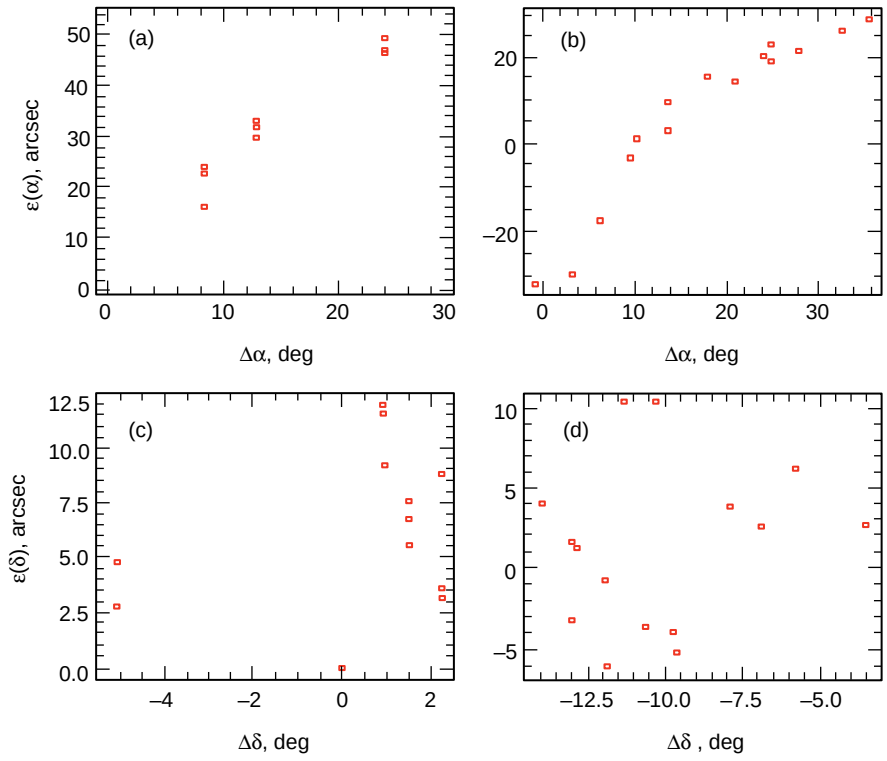

Fig. 1. Star-to-star and star-to-satellite experiments at the 0.6-m telescope: (a) star-to-star RA offset versus RA slew, (b) star-to-satellite RA offset versus RA slew, (c) star-to-star DEC offset versus DEC slew, and (d) star-to-satellite DEC offset versus DEC slew.

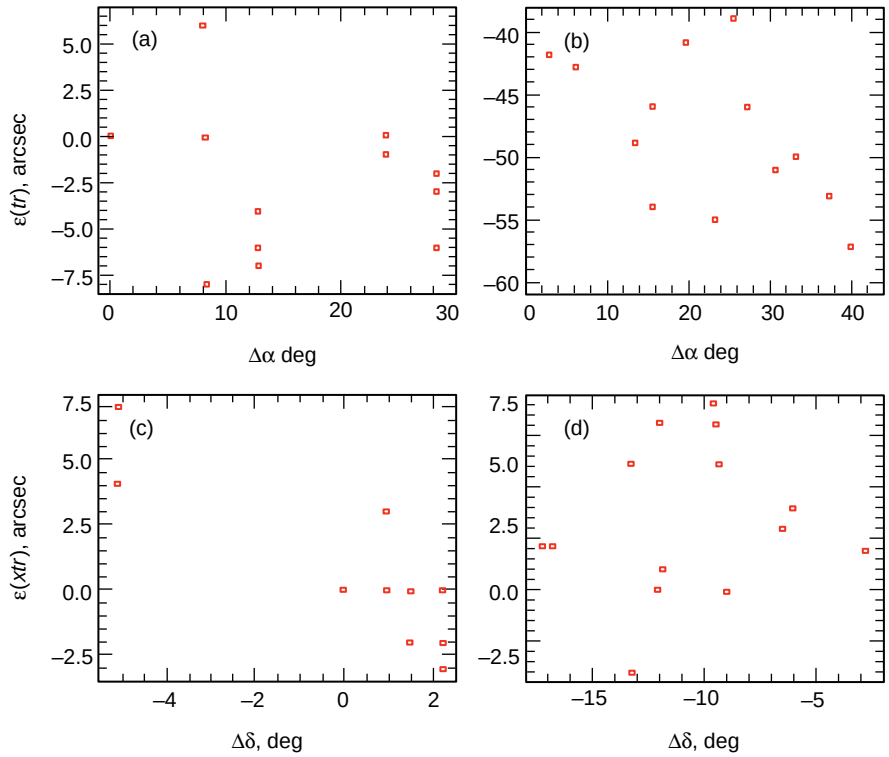

Fig. 2. Star-to-star and star-to-satellite experiments at the 1.2-m telescope: (a) star-to-star track offset versus RA slew, (b) star-to-satellite track offset versus RA slew, (c) star-to-star cross-track offset versus DEC slew, and (d) star-to-satellite cross-track offset versus DEC slew.

The undershoot probably is due to slippage of the declination worm gear along its axis of rotation as it turns. This motion is due to force applied by the bull gear, which meshes with the worm gear [4]. The slippage tends to be always in the direction of motion of the declination axis, and is called end play. Figure 1(c) shows no strong evidence of a trend in declination pointing error with declination slew distance. Errors in this axis were due entirely to end play. Figure 1(d) shows a variation of pointing corrections (offsets) about a mean of zero with an amplitude of a few arcseconds. The magnitude of the errors in Figs. 1(c) and 1(d) are comparable. This indicates that there was no significant error in the satellite's declination as predicted by the ephemeris file.

Figure 2(a) indicates that there was no consistent error in pointing in right ascension at the 1.2-m telescope. Figure 2(b) shows offsets clustered around an average of approximately −50 arcsec. This indicates that the telescope overshot the position of the satellite by an average of 50 arcsec in track during slews varying from 2 to 42 deg. Movement in the track axis is around an azimuth circle with positive track being toward the west. This is, therefore, approximately equal to a right ascension error of −50 arcsec.

The above analysis strongly suggests that both telescopes suffered from pointing errors that were independent of their inherent abilities to point and track. It also indicates that these errors were, at both telescopes, such as to cause them to overshoot in the right ascension direction the actual position of the satellite. The magnitude of the overshoot is seen to be similar at both telescopes.

The 0.6-m and 1.2-m pointing experiments strongly suggest that the ETS-VI ephemeris for May 15, 1996 UT, caused the 0.6-m telescope to undershoot the satellite position by approximately 30 seconds. The version of this ephemeris used at the 1.2-m telescope caused it to undershoot the satellite by a similar amount. Thus, the predicted position of the satellite always was west of the satellite's apparent location

in the sky. The apparent motion of the satellite was from west to east. The above results are consistent with the expectation that the tracking data used to compute the ephemeris would suffer the greatest error along the direction of motion of the satellite. Thus, the ephemeris lagged the apparent motion of the satellite by 30 to 50 arcsec.

The recentering strategy described in Section III was sufficient to compensate for the inherent pointing error of the 0.6-m telescope. A similar strategy used at the 1.2-m telescope. It was sufficient to compensate for the much smaller pointing error there. The box search method described in Section III was used to deal with the ephemeris error. Since this error was statistical in nature, it varied from tracking run to tracking run.

VI. Results of the Pointing Strategies

First, it should be noted that between March 21 and May 26, 1996, bidirectional optical links with the ETS-VI were established on 12 of 16 attempts and one-way transmission only (uplink) was established on 3 of the 16 attempts. Thus, an optical link was established on all but 1 of the 16 opportunities.

The results of the pointing strategies were measured by the success rate in establishing links to the satellite during the day. There were 10 tracking runs between April 26 and May 26, 1996. The satellite was acquired before sunset during seven of these runs. On April 29 and May 23, bidirectional communication was not achieved. Uplink could not be maintained on April 29 because of a sudden change in the condition of the satellite. Downlink could not be established on May 23 because the satellite orientation with respect to the receiver was changing. Bidirectional optical links were established during eight of the runs. In the first successful daytime acquisition (April 26), the link was only momentary, and the downlink was not regained until after dark. The May 26 run was unique. The ETS-VI was acquired approximately 5 hours before dark. A bidirectional link was established approximately 2 hours later and maintained for 2.5 hours, well into the evening. On three occasions (April 26, May 5, and May 8), two-way communications were not established until after dark. In these cases, the satellite was found 16, 34, and 60 arcsec, respectively, from the predicted position. The pointing errors seen on April 26 and May 5 were consistent with the measured inherent pointing errors of the transmitter telescope. The pointing error measured on April 8 was attributable to a 60-arcsec error in the ephemeris.

The experiences cited above and the pointing experiments described in Section V clearly show that errors in the satellite ephemerides and inherent pointing errors of the transmitter telescope were contributing factors in the ability of GOLD to maintain bidirectional communications. Inherent pointing errors were shown to be made up of a component that affected the right ascension pointing in a predictable way and a component due to end play in the declination worm gear that caused the 0.6-m telescope to consistently undershoot the ETS-VI. The results in Section V also show that strategies for acquiring the satellite before dark were very successful.

Since tracking is merely repeated pointing, it is reasonable to suppose that a tracking error would result from a pointing error. A clear trend in pointing error could be seen only in right ascension. The tracking error would manifest as a drift of the satellite in right ascension with a rate proportional to the difference between the apparent rate of motion of the satellite and the rate at which the telescope is being driven. Drifts of the satellite in right ascension as large as 16 arcsec in one-half hour were measured at the 0.6-m telescope on April 2, 1996. The satellite was predicted to be moving at approximately 15 arcsec/s (this was typical of rates near apogee).[4] It would have taken 240 sec to move 1 deg. Based on the results of Section V, an error of 1.7 arcsec in right ascension may have accumulated in that time. Thus, a rate difference of approximately 0.0071 arcsec/s is required to produce a tracking error of 1.7 arcsec over a distance of 1 deg. The sidereal rates of the reference stars depend on their declinations. These varied

[4] W. M. Owen, Jr., "Visibility of ETS-VI From Table Mountain Through September 1996," JPL Interoffice Memorandum 312.8-95-949 (internal document), Jet Propulsion Laboratory, Pasadena, California, December 19, 1995.

from 3.7 to nearly 11 deg (see Table 2). Thus, their sidereal rates varied from 14.7 to 15 arcsec/s. This is more than the rate difference above. No attempt was made on May 15, 1996, to track the satellite or the reference stars for the time required (at least 20 min each) to make accurate estimates of their drift rates. Further work is needed to determine the link between pointing error and tracking error at the 0.6-m telescope. The 1.2-m telescope did not display inherent pointing errors in right ascension or declination. No resulting tracking drifts are expected. Tracking drifts at the 0.6-m telescope probably had the greatest impact on the ability to maintain a bidirectional link because they were large as compared with the 6-arcsec beamwidth of the uplink laser. Manual pointing corrections were made to keep the uplink laser pointed accurately.

References

[1] K. Wilson, M. Jeganathan, J. R. Lesh, J. James, and G. Xu, "Results From Phase-1 and Phase-2 GOLD Experiments," *The Telecommunications and Data Acquisition Progress Report 42-128, October–December 1996*, Jet Propulsion Laboratory, Pasadena, California, pp. 1–11, February 15, 1997. http://tda.jpl.nasa.gov/tda/progress_report/42-128/128K.pdf

[2] W. M. Owen, Jr., "Telescope Pointing for GOPEX," *The Telecommunications and Data Acquisition Progress Report 42-114, April–June 1993*, Jet Propulsion Laboratory, Pasadena, California, pp. 230–233, August 15, 1993.

[3] J. E. Riedel, W. M. Owen, Jr., J. A. Stuve, S. P. Synnott, and R. M. Vaughan, "Optical Navigation During the Voyager Neptune Encounter," AIAA Paper 90-2877, AAS/AIAA Astrodynamics Conference, Portland, Oregon, 1990.

[4] S. D. Gillam, J. W. Young, and D. R. Sidwell, "JPL Table Mountain Facility Support of the Ground/Orbiter Lasercomm Demonstration," *The Telecommunications and Data Acquisition Progress Report 42-125, January–March 1996*, Jet Propulsion Laboratory, Pasadena, California, pp. 1–11, May 15, 1996. http://tda.jpl.nasa.gov/tda/progress_report/42-125/125E.pdf

[5] A. Hirshfeld and R. W. Sinnott, editors, *Sky Catalogue 2000.0*, vol. 1, Cambridge, Massachusetts: Sky Publishing Corp., 1982.